

This is an Open Access document downloaded from ORCA, Cardiff University's institutional repository: <https://orca.cardiff.ac.uk/id/eprint/66236/>

This is the author's version of a work that was submitted to / accepted for publication.

Citation for final published version:

Xiao, Yi, Wan, Liang, Leung, Chi-Sing, Lai, Yukun and Wong, Tien-Tsin 2013. Example-based color transfer for gradient meshes. *IEEE Transactions on Multimedia* 15 (3) , pp. 549-560. 10.1109/TMM.2012.2233725

Publishers page: <http://dx.doi.org/10.1109/TMM.2012.2233725>

Please note:

Changes made as a result of publishing processes such as copy-editing, formatting and page numbers may not be reflected in this version. For the definitive version of this publication, please refer to the published source. You are advised to consult the publisher's version if you wish to cite this paper.

This version is being made available in accordance with publisher policies. See <http://orca.cf.ac.uk/policies.html> for usage policies. Copyright and moral rights for publications made available in ORCA are retained by the copyright holders.



# Example-based Color Transfer for Gradient Meshes

Yi Xiao, Liang Wan, *Member, IEEE*, Chi-Sing Leung, *Member, IEEE*,  
Yu-Kun Lai, and Tien-Tsin Wong, *Member, IEEE*

**Abstract**—Editing a photo-realistic gradient mesh is a tough task. Even only editing the colors of an existing gradient mesh can be exhaustive and time-consuming. To facilitate user-friendly color editing, we develop an example-based color transfer method for gradient meshes, which borrows the color characteristics of an example image to a gradient mesh. We start by exploiting the constraints of the gradient mesh, and accordingly propose a linear-operator-based color transfer framework. Our framework operates only on colors and color gradients of the mesh points and preserves the topological structure of the gradient mesh. Bearing the framework in mind, we build our approach on PCA-based color transfer. After relieving the color range problem, we incorporate a fusion-based optimization scheme to improve color similarity between the reference image and the recolored gradient mesh. Finally, a multi-swatch transfer scheme is provided to enable more user control. Our approach is simple, effective, and much faster than color transferring the rastered gradient mesh directly. The experimental results also show that our method can generate pleasing recolored gradient meshes.

**Index Terms**—Gradient mesh, example-based color transfer, linear operator, PCA-based color transfer

## I. INTRODUCTION

Gradient mesh is a powerful vector graphics representation offered by Adobe Illustrator and Corel Coreldraw. Since it is suited to represent multi-colored objects with smoothly varying colors, many artists use gradient meshes to create photo-realistic vector arts. Based on gradient meshes, image objects are represented by one or more planar quad meshes, each forming a regularly connected grid. Every grid point has the position, color, and gradients of these quantities specified. The image represented by gradient meshes is then determined by bicubic interpolation of these specified grid information.

A photo-realistic gradient mesh is not easy to be created manually. It usually takes several hours even days to create a gradient mesh, because artists have to manually edit the attributes of each grid point. Even for a small gradient

mesh with hundreds of grid points, artists may need to take thousands of editing actions, which is labor intensive. To relieve this problem, several methods for automatic or semi-automatic generation of gradient meshes from a raster image [1], [2] have been developed. Good results can be obtained with the aid of some user assistances. However, how to *efficiently edit* the attributes of gradient meshes is still an open problem.

In this paper, we apply the idea of color transfer to gradient meshes. Specifically, we let users change color appearance of gradient meshes by referring to an example image. Our application is analogous to color transfer on images. But it should be pointed out that a gradient mesh has particular constraints rather than an image. Firstly, a grid point in a gradient mesh not only has color as a pixel does in an image, but also has color gradients defined in parametric domain. Secondly, gradient meshes have grid structures which may be obtained via labor-intensive manual creation and should be maintained during the transfer.

We start our work by analytically investigating the effect of linear operator on colors and color gradients of gradient meshes. Based on our findings, a linear-operator-based color transfer framework is proposed, which allows us to perform color transfer on grid points only. Thanks to the framework, we are able to build our approach on a simple linear color transfer operator, i.e., PCA-based transfer [3]. We then apply an extended PCA-based transfer to handle the color range, and propose a minimization scheme to generate color characteristics more similar to that of the reference image. Afterwards, a gradient-preserving algorithm is optionally performed to suppress local color inconsistency. Finally, we develop a multi-swatch transfer scheme to provide more user control on color appearance. An example with two mesh objects is shown in Figure 1.

The main contribution of our work is a feasible color transfer method that highly exploits the constraints of gradient meshes. Our method is quite simple, parameter-free and requires less user interventions. The only user input is to ask users to specify color swatches. Given an example image, our method is able to produce convincing recolored gradient meshes. Note that our approach is performed on the mesh grids directly. As a result, we can not only maintain the grid structure of gradient meshes, but also achieve fast performance due to the small size of mesh objects.

Copyright (c) 2010 IEEE. Personal use of this material is permitted. However, permission to use this material for any other purposes must be obtained from the IEEE by sending a request to [pubs-permissions@ieee.org](mailto:pubs-permissions@ieee.org).

Y. Xiao and C.S. Leung are with the Department of Electronic Engineering, City University of Hong Kong, Hong Kong. E-mail: [yixiao1984@gmail.com](mailto:yixiao1984@gmail.com), [eeleungc@cityu.edu.hk](mailto:eeleungc@cityu.edu.hk)

L. Wan (corresponding author) is with the School of Computer Software, Tianjin University. E-mail: [lwana@tju.edu.cn](mailto:lwana@tju.edu.cn)

Y.K. Lai is with Cardiff University. E-mail: [yukun.lai@cs.cardiff.ac.uk](mailto:yukun.lai@cs.cardiff.ac.uk)

T.T. Wong is with The Chinese University of Hong Kong. E-mail: [ttwong@cse.cuhk.edu.hk](mailto:ttwong@cse.cuhk.edu.hk)

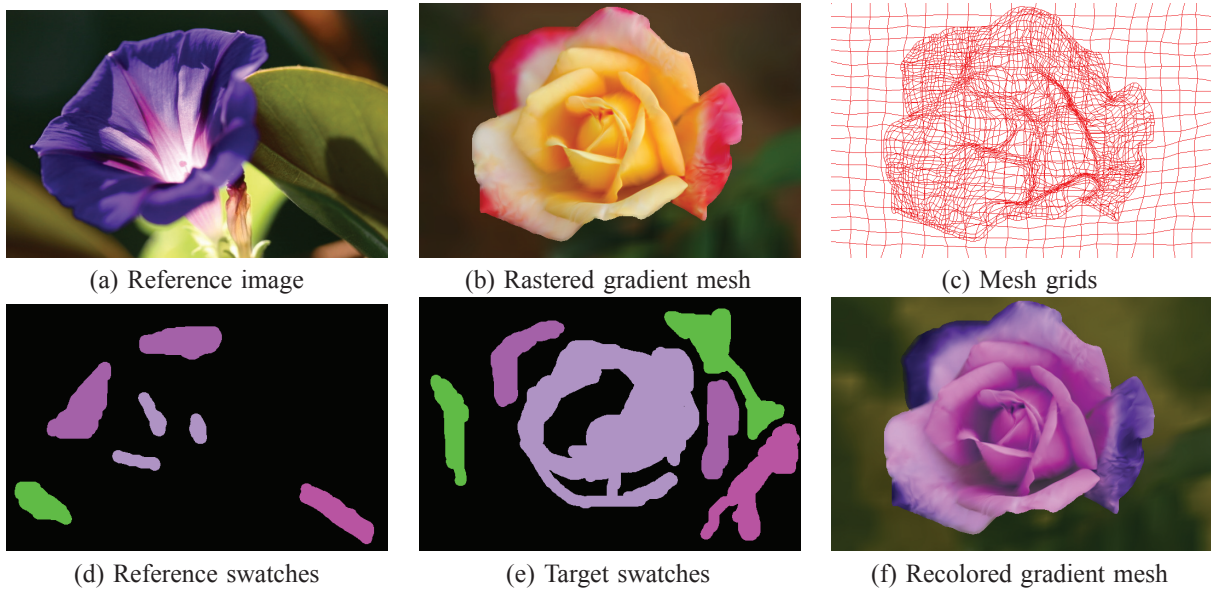


Fig. 1. Color transfer to a gradient mesh by swatches. (a) Reference image. (b) Rastered gradient mesh. (c) The grid structure of the gradient mesh in (b). The gradient mesh consists of two mesh objects. (d) and (e) Specified color swatches for reference image and gradient mesh, respectively. (f) Rastered gradient mesh after color transfer.

## II. RELATED WORK

The concept of color transfer was first introduced by Reinhard et al. [4] to convey the color characteristics of a reference image to a target image. The color distribution of an image is modeled by the mean and standard deviation of color values. Each pixel of the target image is translated and scaled in  $\lambda\alpha\beta$  color space according to the color distributions of the reference and target images. Inspired by this pioneering work, Welsh et al. [5] colorized a grayscale image by borrowing the color characteristics of a color image. Wang and Huang [6] extended [4] to generate an image sequence given an input image and three reference images. Recently, Reinhard and Pouli [7] exploited the impact of color spaces on color transfer effects.

Abadpour and Kasaei [3] modeled the color distribution of an image by the covariance matrix of color values. The color distribution is transferred for each pixel by applying PCA-based transformation. It was proven that the color distribution of the recolored image is the same as that of the reference image when the reference and target images are homogenous. In other words, the reference color distribution can be transferred faithfully. A similar idea was reported in [8][9]. In our work, we will base our gradient mesh recoloring on the method in [3] due to its linearity, simplicity and effectiveness.

It is noted that all the aforementioned methods can produce unnatural looking results when the reference and target images contain different or inhomogeneous color distributions. To address this problem, swatches specified by users are imposed to classify the colors [4][5][3][8]. After locally transferring color distributions between the corresponding swatches, blending the results from each swatch pair yields the final color values. Instead of using a reference image, Levin et al. [10] allowed users to

specify the reference color distribution by drawing color strokes over a grayscale image. They then proposed a global optimization method to diffuse the color strokes across the entire grayscale image. To improve computing efficiency, many succedent methods have been developed [10][11][12][13][14][15]. Recently, An and Pellacini [16] presented a framework to perform color and tone adjustment by using a reference image in a user-controllable manner. Users are asked to specify pair of strokes on reference and targeting images. A non-linear transfer function is computed for each pair of strokes that changes the color distribution of the targeting image to that of the reference image.

Besides interactive color transfer, automatic color transfer has also been addressed. For example, Greenfield and House [17] performed image segmentation, and extracted a color palette by choosing representative colors from the segments. The color mapping between the palettes of the reference and target images is finally computed. Rather than binary segmentation, Tai et al. [18] applied probabilistic segmentation that produces soft region boundaries. Chang et al. [19] categorized each pixel as one of the eleven basic perceptual color categories. Then, color transformation was applied within the same basic color category. This method has been extended to video data [20]. On the other hand, global color mapping techniques based on histogram matching have been developed [21][22]. Recently, Pouli and Reinhard [23] presented a histogram reshaping technique for images of arbitrary dynamic range. Wang et al. [24] developed a training-based method to get both color mapping and gradient mapping for image style and tone transfer. In addition to automatic color transfer between two colorful images, automatic grayscale image colorization methods have been developed, including [25][26][27][28].

Most previous methods handle the target image pixel

by pixel, and may produce spatially inconsistent artifacts. To avoid such artifacts, Xiao and Ma [29] suggested maintaining the fidelity of the target image, i.e., preserving the original gradients. The similar idea can also be found in [30], [31], [32], although expressed in different formulas. As later demonstrated in our paper, we apply a gradient-preserving technique to reduce artifacts due to the minimization scheme for color transfer.

### III. COLOR TRANSFER FOR GRADIENT MESHES

In this section, we first describe the mathematical representation of gradient meshes. Next, we discuss the linear-operator-based color transfer framework. Afterwards, the color transfer with single color swatch is presented in detail. Finally, the color transfer with multiple color swatches is introduced.

#### A. Gradient Mesh

A gradient mesh, as defined in [1][2], is a regularly connected 2D grid. The primitive component of a gradient mesh is a Ferguson patch [33], which is determined by four nearby control points. Each control point specifies three types of information, including position  $\{x, y\}$ , color  $\{r, g, b\}$  and their gradients  $\{m_u, m_v, \alpha m_u, \beta m_v\}$ , where  $m$  is a component of either position or color. The gradients  $m_u$  and  $\alpha m_u$  ( $m_v$  and  $\beta m_v$ ) share the same direction, maintaining continuity between neighboring patches. A Ferguson patch is evaluated via bicubic Hermite interpolation, given by

$$m(u, v) = \mathbf{u}CQC^T\mathbf{v}^T, \quad (1)$$

where

$$Q = \begin{bmatrix} m^0 & m^2 & m_v^0 & m_v^2 \\ m^1 & m^3 & m_v^1 & m_v^3 \\ m_u^0 & m_u^2 & 0 & 0 \\ m_u^1 & m_u^3 & 0 & 0 \end{bmatrix}, C = \begin{bmatrix} 1 & 0 & 0 & 0 \\ 0 & 0 & 1 & 0 \\ -3 & 3 & -2 & -1 \\ 2 & -2 & 1 & 1 \end{bmatrix},$$

the upper script of  $m$  indicates one of the four control points of the Ferguson patch,  $\mathbf{u} = [1 \ u \ u^2 \ u^3]$ ,  $\mathbf{v} = [1 \ v \ v^2 \ v^3]$ , and the parameters have the range of  $0 \leq u, v \leq 1$ . Given an interior point  $(u, v)$ , its positions and colors are calculated using the above equation, respectively. Figure 2 illustrates a gradient mesh with four patches. As shown, the gradient mesh is a compact representation to model image objects with smooth color transitions. Since we only tackle color-related attributes in our application, we regard  $m$  as color in the following.

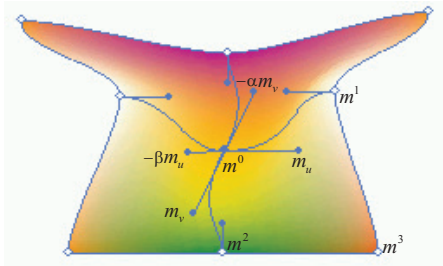


Fig. 2. The gradient mesh contains four Ferguson patches. The gradient information is illustrated for point  $m^0$  in the bottom-right patch.

#### B. Our Framework

Different from raster images, gradient meshes are defined in a parametric domain and have curvilinear grid structures. Since the grid structures should be preserved during the transfer, we aim to perform color transfer in the parametric domain. In other words, we try to tackle colors and color gradients of control points by referring to an example raster image.

We now investigate the properties of colors and color gradients of gradient meshes. As we can see from (1), the color of one point in a Ferguson patch,  $m(u, v)$ , is a *linear combination* of the colors and color gradients of the four control points. When apply a linear operator on  $m(u, v)$ , we get

$$\begin{aligned} am(u, v) + b &= \mathbf{u}CQC^T\mathbf{v}^T + b, \\ &= \mathbf{u}C\hat{Q}C^T\mathbf{v}^T, \end{aligned} \quad (2)$$

where

$$\hat{Q} = \begin{bmatrix} am^0 + b & am^2 + b & am_v^0 & am_v^2 \\ am^1 + b & am^3 + b & am_v^1 & am_v^3 \\ am_u^0 & am_u^2 & 0 & 0 \\ am_u^1 & am_u^3 & 0 & 0 \end{bmatrix}.$$

The above equation tells us that applying a linear operator on color component will be equivalent to applying the linear operator on the colors and color gradients of the control points, respectively, i.e.

$$am(u, v) + b \rightarrow [\{am^i + b\}, \{am_u^i\}, \{am_v^i\}]. \quad (3)$$

Note that the translation item  $b$  is solely applied to the color, while the color gradients are modified just by the scaling item  $a$ . Although (2) is deduced for one color component, it can be extended to a linear combination of three color components as follows,

$$\begin{aligned} am_r(u, v) + bm_g(u, v) + cm_b(u, v) + d \\ \rightarrow \begin{cases} \{am_r^i + bm_g^i + cm_b^i + d\}, \\ \{am_{ur}^i + bm_{ug}^i + cm_{ub}^i\}, \\ \{am_{vr}^i + bm_{vg}^i + cm_{vb}^i\}. \end{cases} \end{aligned} \quad (4)$$

This property reveals that a linear operator is transparent to the parametric interpolation. As a consequence, for an arbitrary point in the gradient mesh, we can just perform a linear color transformation on control points, and do the interpolation as usual. This actually leads to a computational cost depending on the mesh size only and free from the spatial resolution of gradient mesh rasterization.

Based on these findings, we develop a linear-operator-based color transfer framework. It involves two basic steps,

1. An appropriate linear color transformation, i.e., the linear combination parameters  $(a, b, c, d)$ , is determined.
2. The recolored gradient mesh is obtained by updating colors and color gradients of control points according to (4).

The recolored gradient mesh can then be rastered using (1). The proposed framework is subject to the assumption that there is a linear operator being possible to achieve reasonable color transfer. Recall that many methods have been proposed for color transfer between images, ranging

from simple linear operator [5][3][8] to much complicated algorithms [20][26][21][15]. On the other hand, gradient meshes are usually not used to represent natural images with complex scenes. Therefore, we can safely rely on simple yet efficient color transfer methods. To be more specific, we will base our work on PCA-based transformation [3].

### C. Single-Swatch Color Transfer

The basic idea of PCA-based color transfer is to estimate the color characteristics by covariance matrix of colors, and convert colors from the target into the reference color distribution via principal component analysis (PCA). However, using the colors of mesh points alone cannot yield an accurate estimation of color statistics of the gradient mesh. It is also infeasible to compute the covariance matrix analytically. As we always have a raster image  $I_t$  from gradient meshes for preview, we can estimate the color mapping between  $I_t$  and the reference image  $I_r$ .

1) *PCA-based Color Transfer Without Scaling*: Let  $M_t$  and  $M_r$  denote the covariance matrices of  $I_t$  and  $I_r$  in  $RGB$  color space (other color spaces are also applicable). PCA can be done by eigenvalue decomposition of covariance matrix as follows,

$$M = U \cdot \Sigma \cdot U^{-1}. \quad (5)$$

where  $U$  is an orthogonal matrix composed of eigenvectors of  $M$ ,  $\Sigma = \text{diag}(\lambda^R, \lambda^G, \lambda^B)$  containing the eigenvalues of  $M$ . Then the PCA of  $M_t$  and  $M_r$  gives the orthogonal matrices  $U_t$  and  $U_r$ . For the color vector  $c_t$  of a control point, PCA-based color transfer [3] computes the recolored vector  $\tilde{c}$  as

$$\tilde{c} = U_r U_t^{-1} (c_t - \eta_t) + \eta_r, \quad (6)$$

where  $\eta_t, \eta_r$  are the mean color vectors of  $I_t$  and  $I_r$ .

Recall that in addition to colors, our linear-operator-based transfer framework also modifies color gradients. According to (4), the recolored gradient vector of the control point,  $\partial c$ , is computed as

$$\partial \tilde{c} = U_r U_t^{-1} \partial c_t, \quad (7)$$

where  $\partial c_t$  denotes 3-dimensional color gradient vectors in either  $u$  or  $v$  direction. Note that each control point has two gradient vectors and both of them should be transformed.

Figure 3 shows a gradient mesh recolored by (6) and (7) (also referred to *noscale color transfer*). In this example, we convey the color style from the reference image (Figure 3(a)) to the gradient mesh (Figure 3(b), 3(c)). As shown in Figure 3(d), a reasonable result is obtained. The color style of the recolored gradient mesh resembles that of the reference image.

2) *PCA-based Color Transfer With Scaling*: The noscale color transfer only uses the orthogonal matrices  $U_r$  and  $U_t$ . It may sometimes generate colors that go beyond the color range of the reference image  $I_r$ . As shown in Figure 4(d), the color style of the horse becomes too yellowish, and the purple color on the horse head is not in the reference image in Figure 4(a).

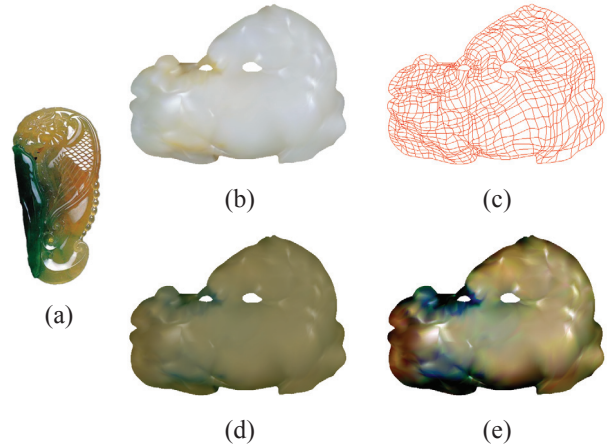


Fig. 3. PCA-based color transfer: (a) Reference image, (b) Rastered gradient mesh, (c) Mesh grids, (d) Color transfer without scaling, (e) Color transfer with scaling. In this example, the scale scheme introduces dark blue colors which are not available in the reference image.

Note that eigenvalue decomposition of  $M_t$  and  $M_r$  also gives two diagonal matrices  $\Sigma_t$  and  $\Sigma_r$ , which contain the eigenvalues of  $M_t$  and  $M_r$ , respectively. The eigenvalues in  $\Sigma_t$  and  $\Sigma_r$  are proportional to the portion of the color “variance” (i.e. the sum of the squared distances of the points from their multidimensional mean). Such variance is related to the color range. To suppress the impact of color range, we may use  $\Sigma_t$  and  $\Sigma_r$  to scale the color vectors as well as the color gradient vectors in the transfer.

Here, we define scale matrix  $S_t = \Sigma_t^{1/2} = \text{diag}(\sqrt{\lambda_t^R}, \sqrt{\lambda_t^G}, \sqrt{\lambda_t^B})$ , and  $S_r = \Sigma_r^{1/2}$ . The square root operator is used to get the standard deviation. The recolored color vector  $\hat{c}$  is then given by

$$\hat{c} = U_r S_r S_t^{-1} U_t^{-1} (c_t - \eta_t) + \eta_r. \quad (8)$$

Similarly, the transformed color derivative vector  $\partial \hat{c}$  is computed as

$$\partial \hat{c} = U_r S_r S_t^{-1} U_t^{-1} \partial c_t. \quad (9)$$

By considering scaling, we can relieve the aforementioned color range problem in some cases. Figure 4(e) shows an example transformed by (8) and (9) (also referred to *scale color transfer*). Compared to 4(d), we found that the purple color is almost removed and the color style looks closer to the reference image in Figure 4(a).

3) *PCA-based Color Transfer with Fusion*: In our experiments, we found the performance of the above two color transfer methods, i.e., noscale and scale, is content-dependent. Figure 4 shows an example favoring the scale scheme. However, in Figure 3, the scale scheme introduces unexpected dark blue on the horse body. There comes out a question that how to choose the transformation. Intuitively, we want to have such a transformation that the resulted color style is as similar to that of the reference image as possible. In this section, we propose a fusion-based minimization scheme to achieve this goal.

Specifically, suppose  $\tilde{c}$  and  $\hat{c}$  are the results of one color transformed by the noscale and scale color transfer, respec-

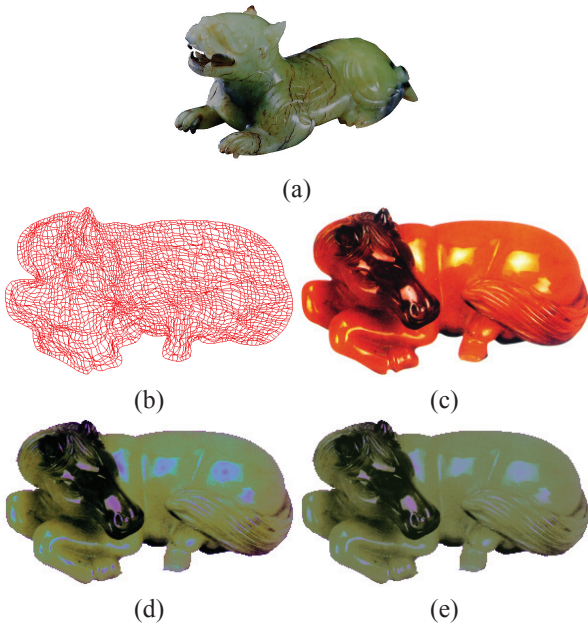


Fig. 4. PCA-based color transfer: (a) Reference Image, (b) Mesh grids, (c) Rastered gradient mesh, (d) Color transfer without scaling, (e) Color transfer with scaling. In this example, the scale scheme suppresses the saturation of purple and blue colors on the horse.

tively. We model the fused color  $c$  by a linear combination of  $\tilde{c}$  and  $\hat{c}$ , given by,

$$c = (1 - k) * \tilde{c} + k * \hat{c}, \quad (10)$$

where  $k \in [0, 1]$  is the weight to be determined. We then measure how similar the fused color is to the color set of  $I_r$ . Here, we adopt Mahalanobis distance and compute it as

$$D(c, I_r) = \sqrt{(c - \eta_r)^T M_r^{-1} (c - \eta_r)}. \quad (11)$$

Note that this fusion model is applied for every pixel in the image independently.

To get the optimal fused color  $c$ , we just need to find the optimal weight  $k^*$ . This can be done by minimizing the distance metric, i.e.,

$$\begin{aligned} k^* &= \min_k D(c, I_r) \\ &= \min_k D((1 - k) * \tilde{c} + k * \hat{c}, I_r). \end{aligned} \quad (12)$$

Since  $D(c, I_r)$  is a quadric function of  $k$ , the minimizing problem can be easily solved. After  $k$  is obtained for one pixel, its fused gradient  $\partial c$  is computed as

$$\partial c = (1 - k) * \partial \tilde{c} + k * \partial \hat{c}. \quad (13)$$

Figure 5 shows the fused results of the two examples used in Figures 3 and 4. In these two examples, the blending factor  $k$  happens to be uniform over the entire image, while  $k = 0$  for Figure 5(a) and  $k = 1$  for Figure 5(b). As a result, the fusion method can avoid artifacts in Figure 3(e) and unexpected colors in Figure 4(d).

In general cases, the fusion-based color transfer can generate spatially varying  $k$  values (see the weight maps in Figures 6(d) and 13(d)). It may sometimes result in quite different transformations for neighboring grid points, and



Fig. 5. Recolored results with our PCA-based fusion method. (a) Fused result of the jade example in Figure 3. (b) Fused result of the horse example in Figure 4.

consequently lead to small artifacts as shown in Figures 6(e) and 6(f). To solve this problem, we adopt a gradient-preserving scheme like [29]. That is, we try to preserve the color differences of the original gradient mesh. To simplify the computation, we just constrain the colors and leave the color gradients intact. Let  $c^*$  denote the final recolored gradient mesh. The gradient-preserving process is modeled as minimizing  $c^*$  from the following equation,

$$c^* = \min_{\tilde{c}} \int_{\Omega} \|\tilde{c} - c\|^2 + \varepsilon \|\nabla \tilde{c} - \nabla c_t\|^2 d\omega, \quad (14)$$

where  $\varepsilon$  is a coefficient for weighting the importance between the color and the color differences between neighboring mesh points.

Figures 6(g) and 6(h) show the gradient-preserving results. Obviously, the artifacts in Figures 6(e) and 6(f) are removed by the gradient-preserving process. This example only contains one gradient mesh. For vector graphics including multiple mesh objects, the gradient-preserving process is applied on each gradient mesh separately.

#### D. Multi-Swatch Color Transfer

So far, we assume the color distribution of either  $I_r$  or  $I_t$  can be modeled by a single Gaussian. When  $I_r$  and  $I_t$  do not work well, we may choose separate color swatch pairs and transfer desired color effects between swatches [4]. This scheme can also provide more flexible user control of color appearance. Some examples can be found in Figures 1 and 7.

For the  $i$ -th pair of swatches, we can obtain the transformed color vector  $c_i$  and transformed gradients vector  $\partial c_i$  using the fusion-based method described in Section III-C3. Here,  $c_i$  are from the fusion step and without undergoing the gradient-preserving process. Also note that the fusion is applied on the  $i$ -th reference swatch rather than the entire reference image. Then the recolored vectors  $c'$  and  $\partial c'$  will be a weighted sum of single-swatch recolored vectors, given by

$$c' = \sum_{i=1}^N w_i c_i, \quad \partial c' = \sum_{i=1}^N w_i \partial c_i, \quad (15)$$

where  $N$  is the number of swatch pairs, and  $w_i$  is a weighting factor that evaluates the importance of an individual swatch pair. Since  $w_i$  is varying for different colors, we have to determine  $w_i$  on-the-fly. Different from [3] in which

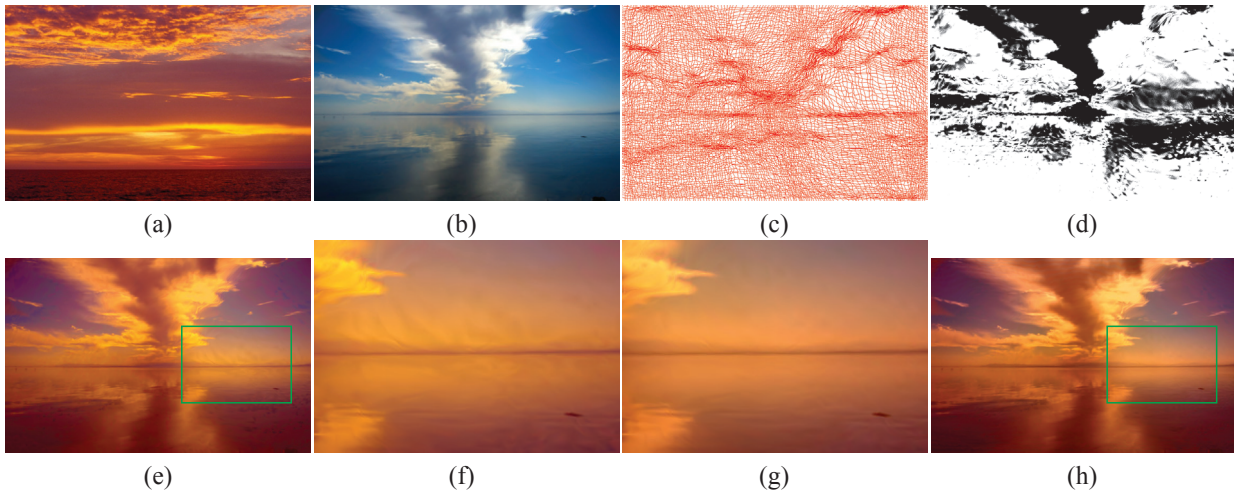


Fig. 6. Color transfer with fusion: (a) Reference image; (b) Rastered gradient mesh; (c) Mesh grids; (d) The weight map in the fusion; (e) Color transfer with fusion alone; (f) Gradient-preserving; The blowups from (e) and (h) are shown in (f) and (g), respectively. The fusion scheme alone may incur small artifacts, while the gradient-preserving process is able to remove the artifacts.

$w_i$  relies on parameter tuning to obtain good results, we determine  $w_i$  automatically as follows

$$w_i = d_i / \sum_{j=1}^N d_j, \quad (16)$$

where  $d_i$  denotes the reciprocal of the Mahalonobis distance from a given color  $c_t$  to a target color swatch  $I_t(i)$ , i.e.,

$$d_i = 1/D(c_t, I_t(i)). \quad (17)$$

It should be noted that the distance calculated here differs from that in the minimization scheme (11). The minimization scheme evaluates the similarity between a transformed color and a color set of the reference image. The multi-swatch blending, however, evaluates the similarity between an original target color and a color set of the target gradient mesh. After the weighting, the gradient-preserving process, if needed, is applied to obtain final results.

Figure 7(f) shows the results of our method. In this example, the purple color of the pitaya, the red color of the apple, and the green color of the two apples are transferred to the red, orange and dark green peppers, respectively. As we can see in Figure 7(f), the colors of recolored peppers resemble those of the reference color swatches faithfully.

#### IV. EXPERIMENTS AND DISCUSSION

We generate gradient mesh vector graphics based on the algorithms from Lai et al. [2] and Sun et al. [1]. For a given raster image, we first apply Lai et al.'s algorithm [2] to create a gradient mesh automatically. In case the quality of the rastered gradient mesh is not very good, we optimize the gradient mesh using Sun et al.'s algorithm [1]. Note that [2] extends the gradient mesh to tolerate image holes. To utilize [1], we decompose one hole-tolerated gradient mesh to two normal meshes at the hole. When the input image is rather complex, the image is first segmented into several parts by manual or automatic methods [34], [35], and each part is approximated by one gradient mesh. Table

I shows the number and size of the gradient meshes and the corresponding rastered images used in the experiments.

##### A. Experimental Results

Figures 1, 3, 4, 6, 7, 9, and 13 demonstrate different examples of recolored gradient meshes by our method. Among these examples, Figures 3, 4 and 6 are created by single-swatch color transfer, the others by multi-swatch color transfer. We use Figures 3 and 4 to compare the performance of color transfer with and without scaling. It is apparent that each transfer method has its applicability. Except for Figures 3 and 4, all the other examples are generated by using the fusion-based color transfer. Also note that only Figure 6 uses the gradient preserving process.

It deserves pointing out that the only user intervention in our system is to specify color swatches. For example, in Figure 1, we use four pairs of color swatches. Two swatches are specified on the flower object, the other two on the background. Both the flower and the background are approximated by one gradient mesh, respectively. In Figures 7 and 9, each of the three peppers is approximated by a single gradient mesh, and just one color swatch is specified for each pepper. As these figures show, the color style of the recolored gradient meshes is quite similar to that of the reference swatches, and the results appear in pleasing visual quality.

##### B. Gradient Mesh v.s. Rastered Gradient Mesh

Now that there is an automatic method [1] to create gradient meshes, readers may think about performing color transfer on the rastered gradient mesh and regenerating the gradient meshes. In the term of timing performance, generating gradient meshes takes about 1 minute on average for examples in the paper. In contrast, recoloring gradient meshes directly spends less than 1 second (more details reported in Section IV-F). On the other hand, we have to note that in many applications keeping the structure of the

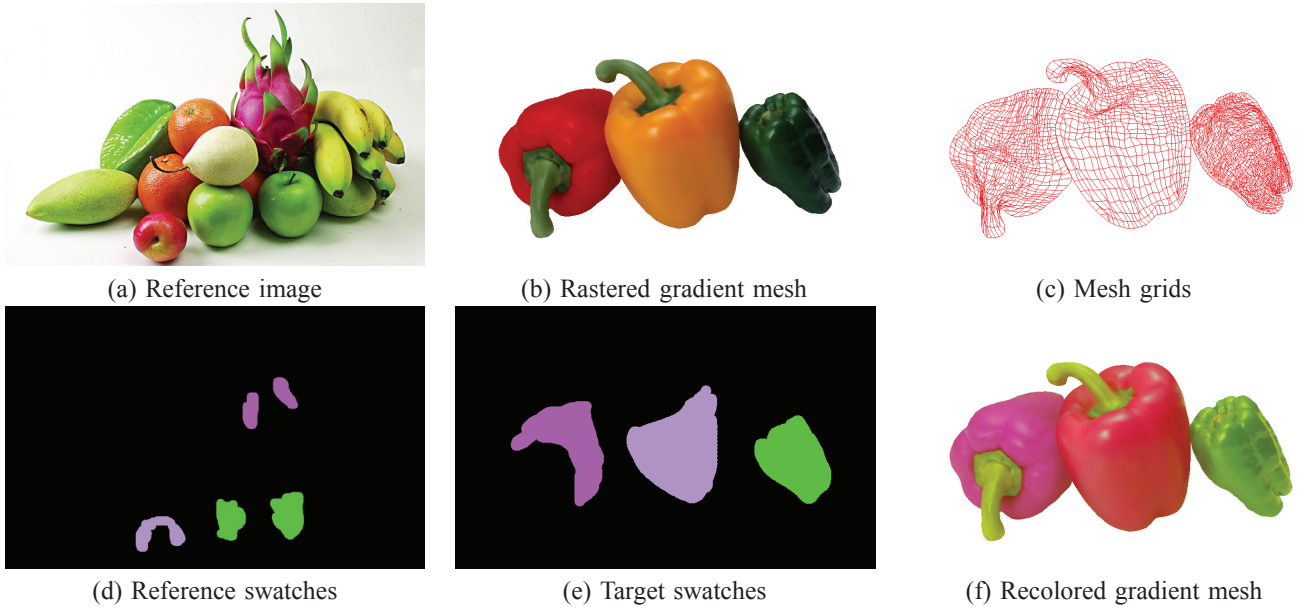


Fig. 7. Color transfer by multi-swatches.

Mesh Name	Meshes	Patches	Resolution
flower (Fig. 1)	2	21×21, 52×63	698 × 464
jade (Fig. 3)	3	28 × 13, 28 × 8, 28×16	600 × 450
horse (Fig. 4)	1	44×78	300 × 174
cloud (Fig. 6)	1	126×127	800 × 511
peppers (Fig. 7)	3	30×33, 26×33, 38×63	800 × 500

TABLE I

THE SIZE OF GRADIENT MESHES AND THE CORRESPONDING RASTER IMAGES USED IN THE EXPERIMENTS.

gradient mesh is important, especially if the structure was originally obtained through labor-intensive manual creation or complicated optimization. The re-vectorization scheme, however, will generally create different mesh structures (readers may compare Figures 12(b) and 12(e)). One reason is that applying the color transfer on the gradient mesh and its raster image may produce different recoloring results. We now make a comparison in the following.

In the case of single swatch, we conduct comparisons for the three color transfer schemes discussed in Section III-C. As we can see in Figure 8, there are nearly no visual differences between the recolored gradient meshes and the recolored raster images for the noscale and scale schemes. This also indicates that transforming a gradient mesh is equivalent to transforming its raster image when using a linear operator. The fusion scheme, on the other hand, introduces a bit larger difference. It is because through the fusion, the neighboring grid points/pixels may have different fusion weights for the noscale and scale schemes. The parametric interpolation then propagates such difference to inner regions inside Ferguson patches.

For the case of multiple swatches, the story is more complicated. The differences between the gradient meshes and the raster images are much larger than those in single swatch case, as shown in Figure 8. It is mainly due to the weighting in multi-swatch color transfer. Since we proceed grid points or pixels separately, neighboring grid points or

pixels may have inconsistent weighting. Consequently, the recolored results of the gradient meshes can be different from that of the raster image. More seriously, transforming on the raster image may introduce obvious artifacts in inner regions. The artifacts can destroy the smooth transition of the gradient mesh. Figure 9 shows an example. In this figure, the black, yellow, and light green colors are transferred to the red, orange, and dark green peppers, respectively. As we can observe in Figure 9(e), there is an unexpected color band near the pepper stem. In contrast, the recolored gradient mesh (see Figure 9(f)) does not have such artifacts, and its color transition still keeps smooth as the original gradient mesh (see Figure 9(b)). The reason for the artifacts is that the pixels in inner regions may be mapped to colors quite different from neighboring pixels. This problem is more likely to appear when the swatches have quite different colors. For gradient meshes, only the colors and gradients of grid points are transformed, which guarantees inner regions have smooth transition.

### C. Comparison of PCA-based Transformations

We now give a quantitative comparison for the three PCA-based transformations discussed in Section III. Similar to [36], we adopt two metrics, colorfulness similarity (CS) between the recolored gradient mesh and the reference image (swatches), and structural similarity (SS) between the recolored image and the target gradient mesh. The

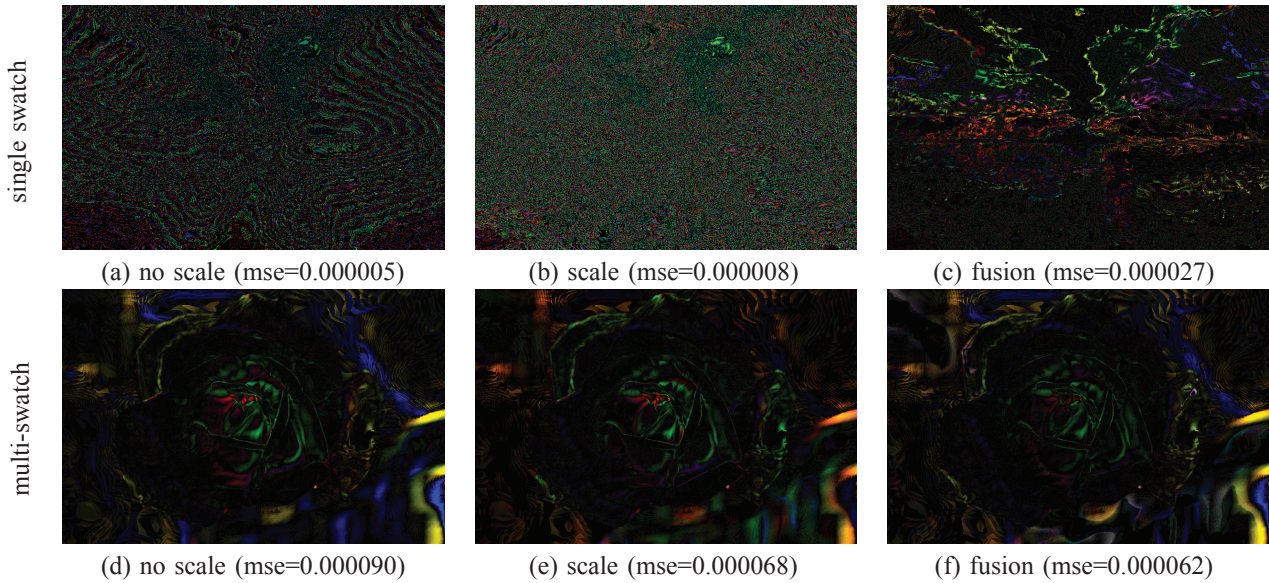


Fig. 8. Difference images between recolored gradient mesh and recolored raster image. The gradient meshes used in the top and bottom row are cloud (Figure 6) and flower (Figure 1), respectively. The difference images are enhanced for comparison purpose.

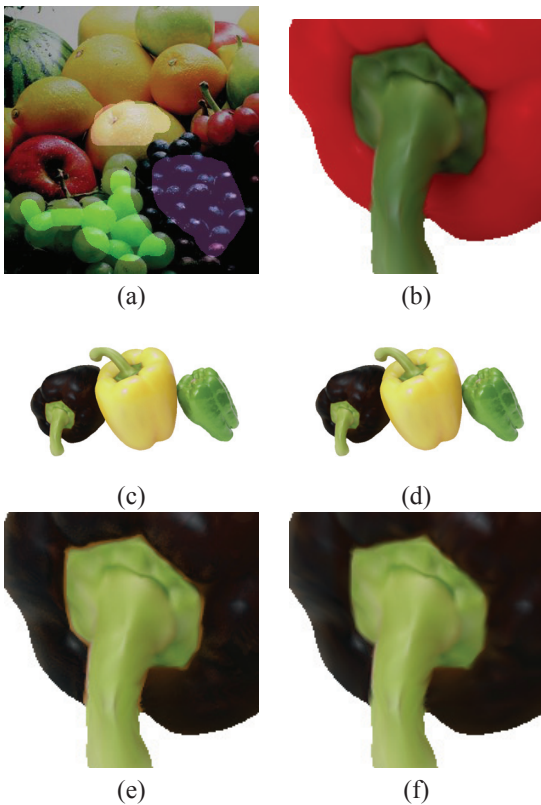


Fig. 9. Transferring on raster images may cause artifacts. (a) Reference image and swatches, (b) Blowup of target gradient mesh, (c) Recolored raster image, (d) Recolored gradient mesh, (e) Blowup of (c), (f) Blowup of (d). Note that, there is an unexpected color band in (e). The target swatches are the same as Figure 7(e).

colorfulness similarity measures the difference of the image's colorfulness [37], while the structural similarity is the mean value of the gradient-based structural similarity (GSSIM) [38] for two images under evaluation. The mathe-

tical definitions can be found in [36]. Instead of using the integrated similarity metric in [36], we compare CS and SS values directly so as to exploit their respective influences. In addition, CS values, which range in  $[0, 109]$ , are normalized to  $[0, 1]$  as SS values. The closer the values approach to 1, the more similar the two images are. In the experiment, we use the raster images of the target and recolored gradient meshes for evaluation. When swatches are specified, only the colors in the reference swatches are counted to calculate the CS values.

Table II lists the metric values of the examples in the paper. As we can see in the table, the SS values are always higher than 0.89 for all the three transformations. That means all the three transformations can well maintain the image structure. For the CS values, both noscale and scale schemes may yield lower values, for example, the jade example in Figure 3 and the flower example in Figure 1. The fusion scheme usually provides a tradeoff between the noscale and scale schemes. It may even improve CS and SS values simultaneously, like the cloud example in Figure 6. We notice in the jade example, the fusion scheme favors the noscale scheme with a lower CS value. The reason is as follows. The fusion scheme minimizes the distance between the recolored vector and the reference color set. The CS metric, on the other hand, measures the standard deviations and mean values of the colors. In the jade example, the scale scheme can create larger standard deviation than the noscale scheme, however, it results in many colors far away from the color distribution of the reference image as shown in Figure 3(e).

#### D. Comparison with Two Possible Solutions

In this section, we compare our current approach with two possible variant solutions. The first variant solution is directly representing the transferred color vector as a linear

Mesh Name	noscale		scale		fusion	
	CS	SS	CS	SS	CS	SS
flower (Fig. 1)	0.8526	0.9285	0.7383	0.9478	0.8378	0.9443
jade (Fig. 3)	0.6907	0.9275	0.9275	0.8926	0.6907	0.9275
horse (Fig. 4)	0.8505	0.9724	0.9999	0.9815	0.9999	0.9815
cloud (Fig. 6)	0.9826	0.9852	0.9530	0.9643	0.9853	0.9862
peppers (Fig. 7)	0.8925	0.9402	0.9246	0.9385	0.9246	0.9385

TABLE II

NUMERICAL EVALUATION OF THE RECOLORED MESHES. CS DENOTES THE COLORFULNESS SIMILARITY, AND SS DENOTES THE STRUCTURAL SIMILARITY. THE HIGHER IS CS/SS, THE MORE SIMILAR THE TWO IMAGES ARE.

combination of the original target color vector, i.e.,

$$\tilde{c} = F(c_t) = A * c_t + b, \quad (18)$$

where  $A$  is a  $3 \times 3$  matrix and  $b$  is a  $3 \times 1$  translation vector. Then we solve for an optimal transformation such that the resulting color distribution becomes similar to the color distribution of the reference image, which can be formulated as the following optimization problem,

$$\min \int_c \|cdf_t(F(c)) - cdf_r(c)\|^2 dc, \quad (19)$$

where  $cdf_t$  and  $cdf_r$  are the cumulative distribution functions of the transferred target image and the reference image, respectively. Then, the transferred gradient vector of gradient meshes can be computed as  $\partial\tilde{c} = A * \partial c_t$ . Figure 10 compares this solution with our approach. The linear combination method generates a result looking similar to ours (in Figure 1(f)). However, it may produce an out-of-gamut color appearance in some regions as shown in Figure 10(d).

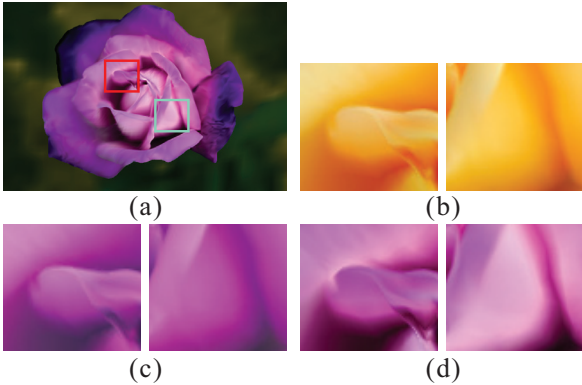


Fig. 10. Our approach v.s. linear combination. (a) the result from the linear combination method. (b-d) show the blowups in the rastered gradient mesh, the results using our approach and the linear combination method, respectively. Note the out-of-gamut color appearance of some regions in the result from the linear combination method.

In the second variant solution, we use an individual weight factor for each color channel in the fusion. That is, we change the single weight in (10) to three weights, i.e.,

$$c = \begin{pmatrix} (1 - k_1) * \tilde{c}_1 + k_1 * \hat{c}_1 \\ (1 - k_2) * \tilde{c}_2 + k_2 * \hat{c}_2 \\ (1 - k_3) * \tilde{c}_3 + k_3 * \hat{c}_3 \end{pmatrix} \quad (20)$$

with  $0 \leq k_1, k_2, k_3 \leq 1$ . Solving for the optimal weight factors for the three color channels can be simply done via

a convex quadratic programming. The transferred gradient vector is then computed in a similar way as (13). We found that for most examples in the paper, the channel-wise weighting scheme and our single weighting scheme get similar results. In the pepper example (see Figure 11), however, the channel wise weighting results in obvious dark artifacts on the left-most pepper, and the stems of the left two peppers look more yellowish. Also note the unexpected ringing appearance on the horse back. In comparison, our single weighting scheme achieves a more pleasing color appearance.

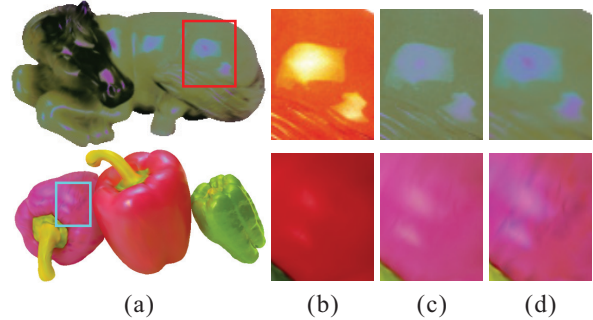


Fig. 11. Our approach v.s. Channel-wise weighting scheme for the fusion. (a) the results from the channel-wise weighting scheme. (b-d) show the blowups in the rastered gradient mesh, the results using our single weighting scheme and the channel-wise weighting scheme, respectively. As shown, the channel-wise weighting may result in inconsistent appearance in some regions.

### E. Comparison with Existing Methods

As aforementioned before, our approach is under the linear-operator-based color transfer framework. Here, we first adopt the linear transformation proposed by Reinhard et al. [4] for comparison. It represents the color distribution by the color mean and standard deviation for each color channel. Note that the RGB-to-Lab color conversion used by their method is nonlinear. Hence, we omit the color conversion and apply the transformation in the RGB color space so as to process the gradients linearly. Figure 12(b) shows the generated result. Compared to our result in Figure 12(a), using mean and standard deviation may generate a weird color appearance.

Next, we experimented with a recently-proposed user-controllable color transfer method [16]. Similar to our approach, this method allows users to specify pairs of strokes to indicate corresponding regions in both the reference and

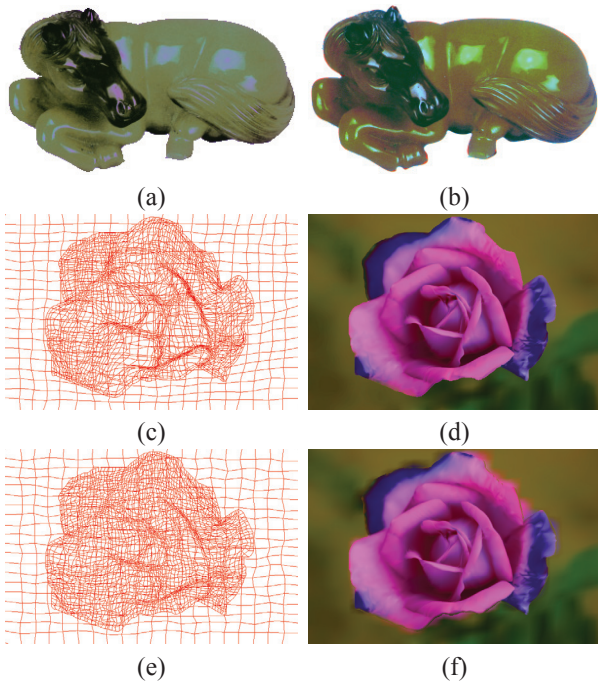


Fig. 12. Comparison with existing methods. (a) and (b) are results using our approach and Reinhard et al’s method [4], respectively. (c) The original gradient meshes for the flower. (d) The recolored raster image using the user-controllable color transfer [16]. (e) The re-generated gradient meshes from (d), which is quite different from the original in (c). (f) The raster image of the updated gradient mesh by resampling color information from (d). In comparison, our approach gets better color appearances in the two examples.

target image. For each stroke pair, a nonlinear constrained parametric transfer model is estimated to do the color transfer. Note that this nonlinear method is not directly applicable to gradient meshes. To make the comparison, we first apply the user-controllable color transfer to the rastered gradient mesh, and then update the gradient mesh by resampling color information from the recolored image (Figure 12(d)). As Lai et al. did in [2], the color gradients are re-estimated using monotonic cubic interpolation [39]. Using the user strokes in Figures 1(d) and 1(e), Figure 12(f) shows the final generated flower result. In comparison with our result in Figure 1(f), the user-controllable method gets more saturated color appearance. More seriously, it may suffer from the problem of color bleeding, for example, in the up-right region of the flower. It is because the geometric positions of gradient meshes are fractional values, and the resampling process may lead to blended colors around mesh boundaries (the flower and the background are separate meshes).

We also regenerate gradient meshes from the recolored image in Figure 12(d) using Lai et al.’s method [2]. Because the gradient mesh is an approximation to the raster image, it inevitably has some loss in image contents. As a result, the mesh regenerated from the recolored image (Figure 12(e)) may be quite different from the original one (Figure 12(c)).

Mesh Name	Gradient Mesh	Raster Image
flower (Fig. 1)	0.875	46.359
jade (Fig. 3)	0.156	3.719
horse (Fig. 4)	0.172	0.984
cloud (Fig. 6)	0.953	11.125
peppers (Fig. 7)	0.735	15.063

TABLE III  
COMPARISONS OF RUNNING TIME (SECONDS) ON GRADIENT MESH AND THE CORRESPONDING RASTER IMAGE.

#### F. Time Performance

Finally, we evaluate the running time of our algorithm in a computer with a Dual-Core Intel 2.2GHz CPU, and 4 GB memory. Our algorithm is implemented in C++. The running time of our algorithm is shown in Table III. The running time is mainly affected by the number of color vectors to be transformed. Therefore, transforming on gradient meshes is much faster than transforming on their raster images due to the smaller size of gradient meshes compared to their raster counterparts. For instance, the cloud example takes about 0.953 seconds for the gradient mesh, just 8.5% of the time duration for the raster image. Meanwhile, since we need to apply our method to a color vector once per swatch pair, the running time is also affected by the number of swatch pairs used. In the flower example (See Figure 1), four swatch pairs are used. The color transfer takes about 0.875 seconds for the gradient mesh and 46.359 seconds for the raster image.

#### V. CONCLUSION

In this paper, we have proposed a simple linear-operator-based color transfer method for gradient meshes. Our method takes reference to a reference image. By exploiting the constraints of gradient meshes, we transfer color characteristics of the reference image to colors and color gradients of control points in gradient meshes. Our method preserves the grid structure of the gradient mesh. In addition to applying PCA-based color transfer to gradient meshes, we investigate the influence of the eigenvalues of the PCA-transform to account for the color range. We further propose a fusion-based minimization scheme to improve the quality of the recolored gradient mesh. To enable more flexible user control of color appearance, a multi-swatch color transfer scheme is developed. Given color swatches, our method is automatic and parameter free. The experimental results shows that our method is very fast and can generate pleasing recolored gradient meshes.

In our current system, users are required to mark color swatches for the color transfer. This provides professional users, like vector graphics artists, intuitive control over the recoloring effect. As our future work, we would like to explore automatic color transfer for gradient meshes, which may be more convenient for amateur users.

#### ACKNOWLEDGMENT

The work was mainly supported by a research grant CityU 116511 (from General Research Fund, Hong Kong).

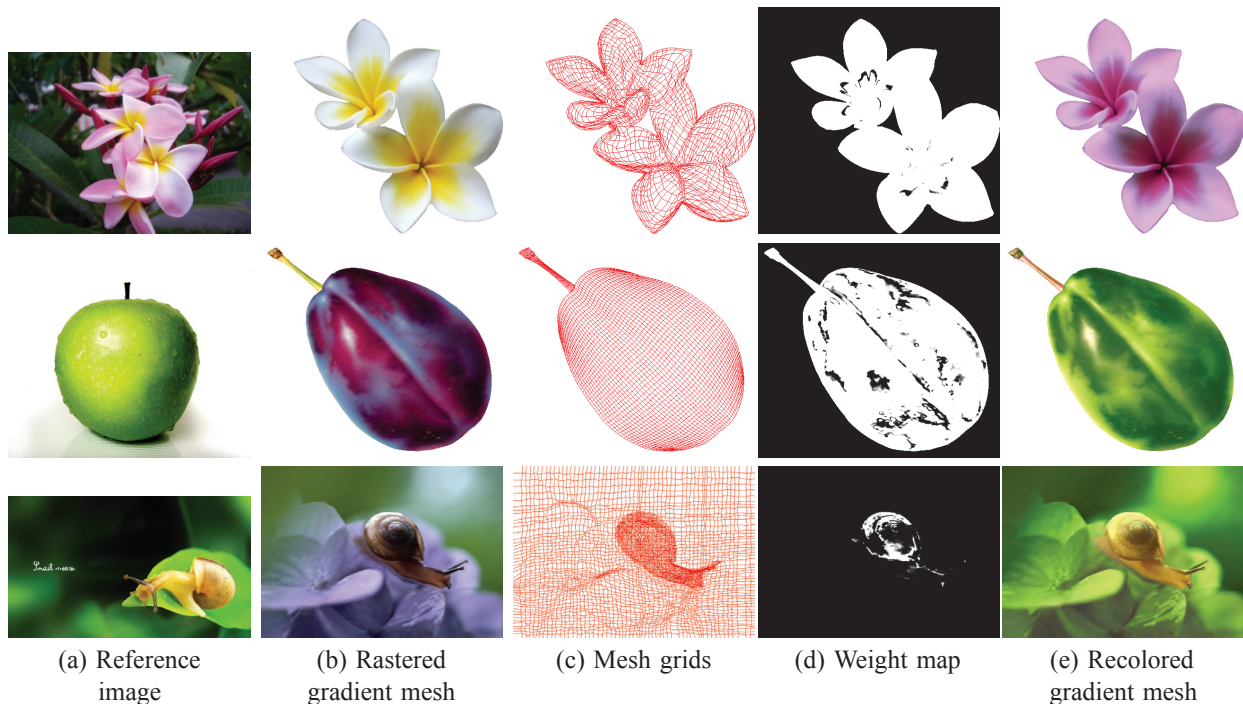


Fig. 13. More results. Note that each stroke pair leads to an individual weight map. Here, we only show one weight map for illustration purpose.

It was partially supported by a research grant SRFDP 20110032120041 (from Specialized Research Fund for the Doctoral Program of Higher Education, China), and a research grant CUHK 417411 (from General Research Fund, Hong Kong).

#### REFERENCES

- [1] J. Sun, L. Liang, F. Wen, and H.-Y. Shum, "Image vectorization using optimized gradient meshes," *ACM Transactions on Graphics*, vol. 26, no. 3, p. 11, 2007.
- [2] Y.-K. Lai, S.-M. Hu, and R. R. Martin, "Automatic and topology-preserving gradient mesh generation for image vectorization," *ACM Transactions on Graphics*, vol. 28, no. 3, pp. 1–8, 2009.
- [3] A. Abadpour and S. Kasaei, "An efficient pca-based color transfer method," *Journal of Visual Communication and Image Representation*, vol. 18, no. 1, pp. 15–34, 2007.
- [4] E. Reinhard, M. Ashikhmin, B. Gooch, and P. Shirley, "Color transfer between images," *IEEE Computer Graphics and Applications*, vol. 21, no. 5, pp. 34–41, 2001.
- [5] T. Welsh, M. Ashikhmin, and K. Mueller, "Transferring color to greyscale images," *ACM Transactions on Graphics*, vol. 21, no. 3, pp. 277–280, 2002.
- [6] C. M. Wang and Y. H. Huang, "A novel color transfer algorithm for image sequences," *Journal of Information Science and Engineering*, vol. 20, no. 6, pp. 1039–1056, 2004.
- [7] E. Reinhard and T. Pouli, "Colour spaces for colour transfer," in *IAPR Computational Color Imaging Workshop*, 2011, pp. 1–15.
- [8] X.-Z. Xiao and L.-Z. Ma, "Color transfer in correlated color space," in *VRCLA '06: Proceedings of the 2006 ACM international conference on Virtual reality continuum and its applications*. New York, NY, USA: ACM, 2006, pp. 305–309.
- [9] H. Kotera, "A scene-referred color transfer for pleasant imaging on display," in *Proceedings of the IEEE International Conference on Image Processing*, 2005, pp. 5–8.
- [10] A. Levin, D. Lischinski, and Y. Weiss, "Colorization using optimization," *ACM Transactions on Graphics*, vol. 23, no. 3, pp. 689–694, 2004.
- [11] T. Horiuchi and H. Kotera, "Colorization for monochrome image with texture," in *Color Imaging Conference*, 2005, pp. 245–250.
- [12] Y.-C. Huang, Y.-S. Tung, J.-C. Chen, S.-W. Wang, and J.-L. Wu, "An adaptive edge detection based colorization algorithm and its applications," in *MM'05: Proceedings of the 13th annual ACM international conference on Multimedia*. New York, NY, USA: ACM, 2005, pp. 351–354.
- [13] L. Yatziv and G. Sapiro, "Fast image and video colorization using chrominance blending," *IEEE Transactions on Image Processing*, vol. 15, no. 5, pp. 1120–1129, 2006.
- [14] Q. Luan, F. Wen, D. Cohen-Or, L. Liang, Y.-Q. Xu, and H.-Y. Shum, "Natural image colorization," in *Rendering Techniques 2007 (Proceedings Eurographics Symposium on Rendering)*, J. Kautz and S. Pattanaik, Eds. Eurographics, June 2007.
- [15] R. Irony, D. Cohen-Or, and D. Lischinski, "Colorization by example," in *Rendering Techniques*, 2005, pp. 201–210.
- [16] X. An and F. Pellacini, "User-controllable color transfer," *Computer Graphics Forum*, vol. 29, no. 2, pp. 263–271, 2010.
- [17] G.-R. Greenfield and D.-H. House, "Image recoloring induced by palette color associations," *Journal of WSCG*, vol. 11, no. 1, pp. 189–196, 2003.
- [18] Y.-W. Tai, J.-Y. Jia, and C.-K. Tang, "Local color transfer via probabilistic segmentation by expectation-maximization," in *CVPR '05: Proceedings of the 2005 IEEE Conference on Computer Vision and Pattern Recognition*, vol. 1. Washington, DC, USA: IEEE Computer Society, 2005, pp. 747–754.
- [19] Y. Chang, S. Saito, and M. Nakajima, "A framework for transfer colors based on the basic color categories," in *CGI2003*. IEEE Computer Society, 2003, pp. 176–183.
- [20] Y. Chang, S. Saito, and M. Nakajima, "Example-based color transformation of image and video using basic color categories," *IEEE Transactions on Image Processing*, vol. 16, no. 2, pp. 329–336, 2007.
- [21] M. Grundland and N. A. Dodgson, "Color histogram specification by histogram warping," in *Processings of the SPIE*, vol. 5667, 2004, pp. 610–624.
- [22] L. Neumann and A. Neumann, "Color style transfer techniques using hue, lightness and saturation histogram matching," in *Proceedings of Computational Aesthetics in Graphics, Visualization and Imaging*, 2005, pp. 111–122.
- [23] T. Pouli and E. Reinhard, "Progressive color transfer for images of arbitrary dynamic range," *Computers and Graphics*, vol. 35, no. 1, pp. 67–80, 2011.
- [24] B. Wang, Y. Yu, and Y.-Q. Xu, "Example-based image color and tone style enhancement," *ACM Transactions on Graphics*, vol. 30, no. 4, pp. 64:1–64:12, July 2011.

- [25] Y. Ji, H.-B. Liu, X.-K. Wang, and Y.-Y. Tang, "Color transfer to greyscale images using texture spectrum," in *Proceedings of the Third International Conference on Machine Learning and Cybernetics*, 2004, pp. 4057 – 4061.
- [26] G. Charpiat, M. Hofmann, and B. Schölkopf, "Automatic image colorization via multimodal predictions," in *Proceedings of the 10th European Conference on Computer Vision*, vol. 3, 2008, pp. 126 – 139.
- [27] J. Li and P. Hao, "Transferring colours to grayscale images by locally linear embedding," in *Proceedings of the British Machine Vision Conference*, 2008, pp. 835 – 844.
- [28] Y. Morimoto, Y. Taguchi, and T. Naemura, "Automatic colorization of grayscale images using multiple images on the web," in *Proceedings of Siggraph Posters*, 2009, p. 32.
- [29] X.-Z. Xiao and L.-Z. Ma, "Gradient-preserving color transfer," *Computer Graphics Forum*, vol. 28, no. 7, pp. 1879–1886, 2009.
- [30] F. Pitié, A. C. Kokaram, and R. Dahyot, "Automated colour grading using colour distribution transfer," *Computer Vision and Image Understanding*, vol. 107, no. 1-2, pp. 123–137, 2007.
- [31] Q. Luan, F. Wen, and Y.-Q. Xu, "Color transfer brush," in *PG '07: Proceedings of the 15th Pacific Conference on Computer Graphics and Applications*. Washington, DC, USA: IEEE Computer Society, 2007, pp. 465–468.
- [32] C.-L. Wen, C.-H. Hsieh, B.-Y. Chen, and M. Ouhyoung, "Example-based multiple local color transfer by strokes," *Computer Graphics Forum*, vol. 27, no. 7, pp. 1765–1772, 2008.
- [33] J. Ferguson, "Multivariable curve interpolation," *J. ACM*, vol. 11, no. 2, pp. 221–228, 1964.
- [34] P. F. Felzenszwalb and D. P. Huttenlocher, "Efficient graph-based image segmentation," *International Journal of Computer Vision*, vol. 59, p. 2004, 2004.
- [35] C. Rother, V. Kolmogorov, and A. Blake, "Grabcut: Interactive foreground extraction using iterated graph cuts," *ACM Transactions on Graphics*, vol. 23, pp. 309–314, 2004.
- [36] Y. Xiang, B. Zou, and H. Li, "Selective color transfer with multi-source images," *Pattern Recognition Letters*, vol. 30, no. 7, pp. 682 – 689, 2009.
- [37] D. Hasler and S. Susstrunk, "Measuring colorfulness in natural images," in *Proc. IS&T/SPIE Electronic Imaging 2003: Human Vision and Electronic Imaging VIII*, vol. 5007, 2003, pp. 87–95.
- [38] Y. C. X. S. Chen, Guan hao, "Gradient-based structural similarity for image quality assessment," in *Proc. of 2006 IEEE International Conference on Image Processing*, 2006, pp. 2929–2932.
- [39] G. Wolberg and I. Alfy, "Monotonic cubic spline interpolation," in *Proc. of Computer Graphics International*, 1999, pp. 188–195.



**Yi Xiao** received the Bachelor's degree and Master's degree in Mathematics from Sichuan University in 2005 and 2008, and the PhD. degree in Electronic Engineering from City University of Hong Kong in 2012. He is currently a Senior Research Associate in the Department of Electronic Engineering, City University of Hong Kong. His research interests include Neural Networks and Computer graphics.



**Liang Wan** received the B.Eng and M.Eng degrees in computer science and engineering from Northwestern Polytechnical University, P.R. China, in 2000 and 2003, respectively. She obtained a Ph.D. degree in computer science and engineering from The Chinese University of Hong Kong in 2007. She is currently an Associate Professor in the School of Computer Software, Tianjin University, P. R. China. Her research interest is mainly on computer graphics, including image-based rendering, non-photorealistic rendering, pre-computed lighting, and image processing.



**Chi-Sing Leung** received the B.Sci. degree in electronics, the M.Phil. degree in information engineering, and the PhD. degree in computer science from the Chinese University of Hong Kong in 1989, 1991, and 1995, respectively. He is currently an Associate Professor in the Department of Electronic Engineering, City University of Hong Kong. His research interests include neural computing, data mining, and computer graphics. In 2005, he received the 2005 IEEE Transactions on Multimedia Prize Paper Award for his paper titled, "the Plenoptic Illumination Function" published in 2002. He is the Program Chair of ICONIP2009. He is also a governing board member of the Asian Pacific Neural Network Assembly (APNNA).



**Yu-Kun Lai** received his bachelor's degree and PhD degree in computer science from Tsinghua University in 2003 and 2008, respectively. He is currently a lecturer of visual computing in the School of Computer Science and Informatics, Cardiff University, Wales, UK. His research interests include computer graphics, geometry processing, image processing and computer vision.



**Tien-Tsin Wong** received the B.Sci., M.Phil., and Ph.D. degrees in computer science from the Chinese University of Hong Kong in 1992, 1994, and 1998, respectively. Currently, he is a Professor in the Department of Computer Science & Engineering, The Chinese University of Hong Kong. His main research interest is computer graphics, including perception graphics, computational manga, image-based rendering, GPU techniques, natural phenomena modeling, and multimedia data compression. He received IEEE Transactions on Multimedia Prize Paper Award 2005, Young Researcher Award 2004. He is also the awardee of National Thousand Talents Plan of China 2011.